

Rare decays $B_s \rightarrow l^+l^-$ and $B \rightarrow Kl^+l^-$ in the topcolor-assisted technicolor model

Wei Liu, Chong-Xing Yue, and Hui-Di Yang

*Department of Physics, Liaoning Normal University, Dalian 116029, China**

(Received 19 October 2008; revised manuscript received 18 January 2009; published 10 February 2009)

We examine the rare decays $B_s \rightarrow l^+l^-$ and $B \rightarrow Kl^+l^-$ in the framework of the topcolor-assisted technicolor (TC2) model. The contributions of the new particles predicted by this model to these rare decay processes are evaluated. We find that the values of their branching ratios are larger than the standard model predictions by one order of magnitude in wide range of the parameter space. The longitudinal polarization asymmetry of leptons in $B_s \rightarrow l^+l^-$ can approach $\mathcal{O}(10^{-2})$. The forward-backward asymmetry of leptons in $B \rightarrow Kl^+l^-$ is not large enough to be measured in future experiments. We also give some discussions about the branching ratios and the asymmetry observables related to these rare decay processes in the lightest Higgs model with T-parity.

DOI: 10.1103/PhysRevD.79.034008

PACS numbers: 13.20.He

I. INTRODUCTION

The study of pure leptonic and semileptonic decays of B meson is one of the most important tasks of B physics both theoretically and experimentally. These rare B decays are sensitive to new physics (NP) and their signals are useful for testing the standard model (SM) [1]. So far, a lot of works have been concentrated on these decays. In the SM, there are no flavor changing neutral current (FCNC) processes at the tree level and the leading contributions to these decays come from the one-loop level. So these rare decays are rather sensitive to the contributions from the NP models beyond the SM. Studying of the observables of the asymmetries, such as the CP asymmetry [2], longitudinal polarization (LP) asymmetry A_{LP} [3], and forward-backward (FB) asymmetry A_{FB} [4] etc, interests experiments in testing NP. Certainly, their detection requires excellent triggering and identification of leptons with low misidentification rates for hadrons. The precision measurement needs further studying.

The quark level transition $b \rightarrow sl^+l^-$ is responsible for both the purely leptonic decays $B_s \rightarrow l^+l^-$ and the semileptonic decays $B \rightarrow Kl^+l^-$ ($l = e, \mu, \tau$). The decay $B_s \rightarrow \mu^+\mu^-$ will be one of the most important rare B decays to be studied at the upcoming large hadron collider (LHC), and so far the upper bound on its branching ratio is [5]

$$\text{Br}(B_s \rightarrow \mu^+\mu^-) < 5.8 \times 10^{-8} (95\% \text{ C.L.}). \quad (1)$$

The branching ratios of $B \rightarrow Kl^+l^-$ observed by BABAR collaboration and Belle collaboration are [6,7]

$$\text{Br}(B \rightarrow Kl^+l^-) = (5.7_{-1.8}^{+2.2}) \times 10^{-7}, \quad (2)$$

which is close to the SM prediction [1,8]. However, due to the errors in the determination of the hadronic form factors

and the Cabibbo-Kobayashi-Maskawa (CKM) matrix element $|V_{ts}|$, there is about 20% uncertainty in SM prediction. The experimental measurement values of rare decay processes $B_s \rightarrow e^+e^-, \tau^+\tau^-$ will be discussed later.

We also consider other observables of the purely leptonic and semileptonic decays for the B meson, which are sensitive to scalar/pseudoscalar new physics (SPNP) contributions to $b \rightarrow s$ transitions. They are forward-backward asymmetry A_{FB} of leptons in $B \rightarrow Kl^+l^-$ and longitudinal polarization asymmetry A_{LP} of leptons in $B_s \rightarrow l^+l^-$. The observable A_{LP} was introduced in Ref. [3], though the corresponding analysis in the context of $K \rightarrow \mu^+\mu^-$ had been carried out earlier [9]. The average A_{FB} in the rare decay processes $B \rightarrow Kl^+l^-$ has been measured by BABAR collaboration as [6]

$$\langle A_{FB} \rangle = 0.15_{-0.23}^{+0.21} \pm 0.08. \quad (3)$$

This measured value is close to zero and has a high experimental error. As the values of A_{LP} and A_{FB} predicted in the SM are nearly zero, any nonzero value of one of these asymmetries is a signal for NP. This is the main reason we focus on these observables.

In literature, there are numerous studies of the quark level decays $b \rightarrow sl^+l^-$ both in the SM and in some NP models. Recently, Refs. [10,11] have studied the sensitivity of these rare decay processes to the radius R in the universal extra dimension (UED) model. In the supersymmetry (SUSY) models, extensive works have been taken to the branching ratios of these rare decays, and some of these discussions are related to the asymmetry aspect [12,13]. These decays have also been discussed in the lightest Higgs model with T-parity (called the LHT model) [14], they have verified that the LHT model can enhance the branching ratios of these decays [15]. However, they have not discussed the asymmetry observables, we will give some

*cxyue@lnnu.edu.cn

discussions on these observables in the framework of the LHT model.

In the framework of the topcolor-assisted technicolor (*TC2*) model [16], Ref. [17] has calculated the branching ratios of quark level $b \rightarrow sl^+l^-$ decays. They consider the contributions of the non-universal gauge boson Z' predicted by this model. Their numerical results show that the enhancement is quite large when the mass of Z' is small. Reference [18] has calculated the contributions coming from the pseudoscalar top-pions predicted by this model to the branching ratios of the decays $B_s \rightarrow l^+l^-$. Reference [19] has evaluated the contributions from both the neutral and charged scalars predicted by this model, the branching ratios can be enhanced over the SM predictions by two orders of magnitude in some part of parameter space. So far, we have not seen the study of the asymmetry observables for these two decays in the framework of the *TC2* model, and furthermore the former discussions on the branching ratios have not considered the contributions induced by all the particles predicted by this model.

In this paper, we consider the contributions coming from all of the new particles predicted by the *TC2* model to the branching ratios and asymmetries related to the rare decay processes $b \rightarrow sl^+l^-$. Compared with the predictions in the SM, our results show that the contributions to the branching ratios and the asymmetries come from two aspects. First, the Wilson coefficients of these processes receive additional contributions from the nonuniversal gauge boson Z' and charged top-pions. Second, the neutral top-pion and top-Higgs can give contributions through newly introduced scalar/pseudoscalar operators. For comparison, we also give our results in the LHT model, considering different parametrization scenarios.

This paper is arranged as follows. In the following section, we will summarize some elementary features of the *TC2* model. In Sec. III we present our calculation on the decay processes $B_s \rightarrow l^+l^-$. The decay processes $B \rightarrow Kl^+l^-$ will be studied in the Sec. IV. In Sec. V we give simple discussions on the above questions in the LHT model. Conclusions are given in Sec. VI.

II. THE *TC2* MODEL

The *TC2* model [16] is one kind of the phenomenological viable models, which has all essential features of the topcolor scenario. The *TC2* model generates the large quark mass through the formation of a dynamical $t\bar{t}$ condensation and provides possible dynamical mechanism for electroweak symmetry breaking (EWSB). The physical top-pions ($\pi_i^{0,\pm}$), the nonuniversal gauge boson (Z'), and the top-Higgs (h_i^0) are predicted. The presence of the physical top-pions $\pi_i^{0,\pm}$ in the low energy spectrum is an inevitable feature of the topcolor scenario, regardless of the dynamics responsible for EWSB and other quark mass. The flavor-diagonal (FD) couplings of top-pions to fermions can be written as [16,20]:

$$\begin{aligned} & \frac{m_i^*}{\sqrt{2}F_t} \frac{\sqrt{v_w^2 - F_t^2}}{v_w} [i\bar{l}\gamma^5 t \pi_i^0 + \sqrt{2}\bar{l}_R b_L \pi_i^+ + \sqrt{2}\bar{b}_L t_R \pi_i^-] \\ & + \frac{m_b^*}{\sqrt{2}F_t} [i\bar{b}\gamma^5 b \pi_i^0 + \sqrt{2}\bar{l}_L b_R \pi_i^+ + \sqrt{2}\bar{b}_R t_L \pi_i^-] \\ & + \frac{m_l}{v} \bar{l}\gamma^5 l \pi_i^0, \end{aligned} \quad (4)$$

where $m_i^* = m_i(1 - \varepsilon)$, $v_w = v/\sqrt{2} = 174$ GeV, $F_t \approx 50$ GeV is the top-pion decay constant. The ETC interactions give rise to the masses of the ordinary fermions including a very small portion of the top quark mass, namely εm_t with a model dependent parameter $\varepsilon \ll 1$, and $m_b^* = m_b - 0.1\varepsilon m_t$ [21]. The factor $\frac{\sqrt{v_w^2 - F_t^2}}{v_w}$ reflects mixing effect between top-pions and the Goldstone bosons.

For the *TC2* model, the underlying interactions, topcolor interactions, are nonuniversal and therefore do not possess Glashow-Iliopoulos-Maiani (GIM) mechanism [22]. One of the most interesting features of $\pi_i^{0,\pm}$ is that they have large Yukawa couplings to the third-generation quarks and can induce the tree-level flavor changing (FC) couplings [23,24]. When one writes the nonuniversal interactions in the quark mass eigen-basis, it can induce the tree-level FC couplings. The FC couplings of top-pions to quarks can be written as [17,23]:

$$\begin{aligned} & \frac{m_t}{\sqrt{2}F_t} \frac{\sqrt{v_w^2 - F_t^2}}{v_w} [iK_{UR}^{tc} K_{UL}^{t*} \bar{l}_L c_R \pi_i^0 \\ & + \sqrt{2}K_{UR}^{tc} K_{DL}^{bb} \bar{c}_R b_L \pi_i^+ + \sqrt{2}K_{UR}^{tc} K_{DL}^{bb*} \bar{b}_L c_R \pi_i^- \\ & + \sqrt{2}K_{UR}^{tc} K_{DL}^{ss} \bar{l}_R s_L \pi_i^+ + \sqrt{2}K_{UR}^{tc} K_{DL}^{ss*} \bar{s}_L t_R \pi_i^-], \end{aligned} \quad (5)$$

where $K_{UL(R)}$ and $K_{DL(R)}$ are rotation matrices that diagonalize the up-quark and down-quark mass matrices M_U and M_D , i.e., $K_{UL}^{tc} M_U K_{UR} = M_U^{dia}$ and $K_{DL}^{tc} M_D K_{DR} = M_D^{dia}$, for which the CKM matrix is defined as $V = K_{UL}^{tc} K_{DL}$. To yield a realistic form of the CKM matrix V , it has been shown that the values of the coupling parameters can be taken as [23]:

$$K_{UL}^{tt} \approx K_{DL}^{bb} \approx K_{DL}^{ss} \approx 1, \quad K_{UR}^{tc} \leq \sqrt{2\varepsilon - \varepsilon^2}. \quad (6)$$

In the following calculation, we will take $K_{UR}^{tc} = \sqrt{2\varepsilon - \varepsilon^2}$ and take ε as in the range of 0.03–0.1 [16]. The *TC2* model predicts the existence of the top-Higgs h_i^0 , which is a $t\bar{t}$ bound and analogous to the σ particle in low energy QCD. It has similar Feynman rules as the SM Higgs boson, so we do not list them.

Another significant feature of the *TC2* model is the existence of nonuniversal gauge boson Z' , which may provide significant contributions to some FCNC processes because of its FC couplings to fermions. The FC $b - s$ coupling to Z' can be written as [25]:

$$\mathcal{L}_{Z'}^{\text{FC}} = -\frac{g_1}{2} \cot\theta' Z'^\mu \left\{ \frac{1}{3} D_L^{bb} D_L^{b_s^*} \bar{s}_L \gamma_\mu b_L - \frac{2}{3} D_R^{bb} D_R^{b_s^*} \bar{s}_R \gamma_\mu b_R + \text{H.c.} \right\}, \quad (7)$$

D_L, D_R are matrices which rotate the down-type left and right hand quarks from the quark field to mass eigen-basis. The FD couplings of Z' to fermions, which are relative to our calculation, can be written as [16,17,20,26]:

$$\mathcal{L}_{Z'}^{\text{FD}} = -\sqrt{4\pi K_1} \left\{ Z'_\mu \left[\frac{1}{2} \bar{\tau}_L \gamma^\mu \tau_L - \bar{\tau}_R \gamma^\mu \tau_R + \frac{1}{6} \bar{l}_L \gamma^\mu t_L + \frac{1}{6} \bar{b}_L \gamma^\mu b_L + \frac{2}{3} \bar{t}_R \gamma^\mu t_R - \frac{1}{3} \bar{b}_R \gamma^\mu b_R \right] - \tan^2\theta' Z'_\mu \left[\frac{1}{6} \bar{s}_L \gamma^\mu s_L - \frac{1}{3} \bar{s}_R \gamma^\mu s_R - \frac{1}{2} \bar{\mu}_L \gamma^\mu \mu_L - \frac{1}{2} \bar{\mu}_R \gamma^\mu \mu_R - \frac{1}{2} \bar{e}_L \gamma^\mu e_L - \bar{e}_R \gamma^\mu e_R \right] \right\}, \quad (8)$$

where K_1 is the coupling constant and θ' is the mixing angle with $\tan\theta' = \frac{g_1}{\sqrt{4\pi K_1}}$. g_1 is the ordinary hypercharge gauge coupling constant.

In the following sections, we will use the above formulas to calculate the contributions of the $TC2$ model to the rare decay processes $B_s \rightarrow l^+ l^-$ and $B \rightarrow Kl^+ l^-$.

III. THE CONTRIBUTIONS OF THE $TC2$ MODEL TO THE RARE DECAY PROCESSES $B_s \rightarrow l^+ l^-$

The $TC2$ model can give contributions to rare B decays two different ways, either through the new contributions to the Wilson coefficients or through the new scalar or pseudoscalar operators. The most general model independent form of the effective Hamilton for the decays $B_s \rightarrow l^+ l^-$ including the contributions of NP has the form:

$$H(B_s \rightarrow l^+ l^-) = H_0 + H_1 \quad (9)$$

with

$$H_0 = \frac{\alpha G_F}{2\sqrt{2}\pi} (V_{ts}^* V_{tb}) \{ R_A (\bar{s} \gamma_\mu \gamma_5 b) (\bar{l} \gamma^\mu \gamma_5 l) \}, \quad (10)$$

$$H_1 = \frac{\alpha G_F}{\sqrt{2}\pi} (V_{tb} V_{ts}^*) \{ R_S (\bar{s} P_R b) (\bar{l} l) + R_P (\bar{s} P_R b) (\bar{l} \gamma_5 l) \}. \quad (11)$$

Where H_0 represents the SM operators and H_1 represents the SPNP operators. Here $P_{L,R} = (1 \mp \gamma_5)/2$, R_S, R_P , and R_A denote the strengths of the scalar, pseudoscalar, and axial vector operators, respectively [27]. In our analysis we assume that there are no additional CP phases apart from the single CKM phase, thus R_S and R_P are real. In the SM, the scalar and pseudoscalar couplings R_S and R_P receive contributions from the penguin diagrams with physical and unphysical neutral scalar exchange and are highly suppressed to $\mathcal{O}(10^{-5})$. The coupling constant of the axial

vector operator R_A can be expressed as $R_A = Y^{\text{SM}}(x)/\sin^2\theta_W$, where $Y^{\text{SM}}(x)$ is the SM Inami-Lim function [28], which has been listed in Appendix A. These coupling constants will receive contributions coming from the nonuniversal gauge boson Z' and the scalars $\pi_i^{0,\pm}, h_i^0$.

A. The contributions of the nonuniversal gauge boson Z'

In the $TC2$ model, the nonuniversal gauge boson Z' can give corrections to the SM function $Y(x)$, which directly determine the coupling constant R_A . The relevant Feynman diagrams have been shown in Fig. 1. In these diagrams, the Goldstone boson ϕ is introduced by the 't Hooft-Feynman gauge, which can cancel the divergence in self-energy diagrams. Because the couplings of $Z'WW$, $Z'\phi\phi$ and $Z'W\phi$ do not exist in the $TC2$ model, the diagrams that including the above couplings are not present. The small interference effects between Z' and Z are not considered here. In this situation, the function $Y^{TC}(x_l)$ for $l = e, \mu$ is obtained as follows:

$$Y^{TC}(x_l) = \frac{-\tan^2\theta' M_Z^2}{M_{Z'}^2} (C_{ab}(x_l) + C_c(x_l) + C_d(x_l)), \quad (12)$$

here $x_l = m_l^2/M_W^2$. The factor $-\tan^2\theta'$ does not exist for the decay process $B_s \rightarrow \tau^+ \tau^-$ which can be seen from Eq. (8). The formations of $C_{ab}(x_l)$, $C_c(x_l)$, and $C_d(x_l)$ can be easily obtained in the framework of the $TC2$ model using the method in Ref. [28]. The detailed expression forms of these functions are listed in the Appendix B.

The nonuniversal gauge boson Z' has FC coupling with fermions as shown in Eq. (7), the tree level Feynman diagram contributing to the decay processes $B_s \rightarrow l^+ l^-$

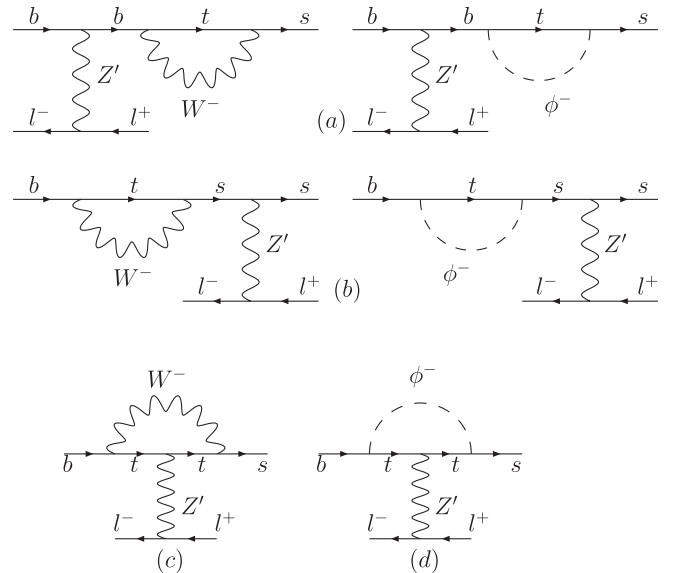


FIG. 1. Penguin diagrams of Z' contributing to $B_s \rightarrow l^+ l^-$ in the $TC2$ model.

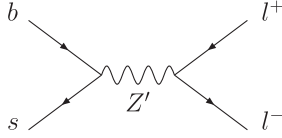


FIG. 2. Tree-level diagram of Z' contributing to $B_s \rightarrow l^+ l^-$ within the $TC2$ model.

has been shown in Fig. 2. The contributions can be obtained by directly calculating Fig. 2 using the standard method in Ref. [25], and the B_s width can be written as:

$$\Gamma(B_s \rightarrow l^+ l^-) = \frac{1}{4608\pi} f_{B_s}^2 m_{B_s} m_l^2 \sqrt{1 - \frac{4m_l^2}{m_{B_s}^2} \delta_{bs}^2} \times \cot^2 \theta' X^2(\theta') \left(\frac{g_1}{M_{Z'}} \right)^4, \quad (13)$$

where

$$\delta_{bs} = D_L^{bb} D_L^{bs*} + 2D_R^{bb} D_R^{bs*}. \quad (14)$$

$X(\theta') = \cot \theta'$ for $l = \tau$, and $X(\theta') = \tan \theta'$ for $l = e$ and μ . f_{B_s} is the decay constant of B_s meson.

B. The contributions of the scalars ($\pi_t^{0,\pm}, h_t^0$)

The scalars predicted by the $TC2$ model give contributions to the decay processes $B_s \rightarrow l^+ l^-$ through corrections to the coupling constants in Eq. (10) and (11). The relevant Feynman diagrams are displayed in Fig. 3, in which (a) shows the contributions of neutral top-Higgs h_t^0 and top-pion π_t^0 to the couplings R_S and R_P , respectively; (b), (c), and (d) show the contributions of the charged top-pions π_t^\pm to the coupling R_A . The expression of the coefficient R_S can be written as:

$$R_S = \frac{m_b^* m_l \nu \sqrt{\nu_w^2 - F_\pi^2}}{2\sqrt{2} m_{h_t^0}^2 F_\pi \nu_w \sin^2 \theta_w} C(x_t) + \frac{m_b^* m_l m_t M_W^2 V_{ts} \sqrt{\nu_w^2 - F_\pi^2}}{4\sqrt{2} m_{h_t^0}^2 F_\pi^2 \nu_w g_2^4} C(x_s). \quad (15)$$

Here $x_s = m_t^*/M_S^2$, M_S is the mass of the top-pions. $C(x_t)$ is the Inami-Lim function in the SM [28]. Since the neutral top-Higgs coupling with fermions is different from that of neutral top-pion by only a factor of γ_5 , the expression of R_P is same as that of R_S except only for the masses of the scalar particles. In our numerical estimation, we will take $m_{\pi_t^0} = m_{h_t^0} = M_S$. In this case, $R_P = R_S$.

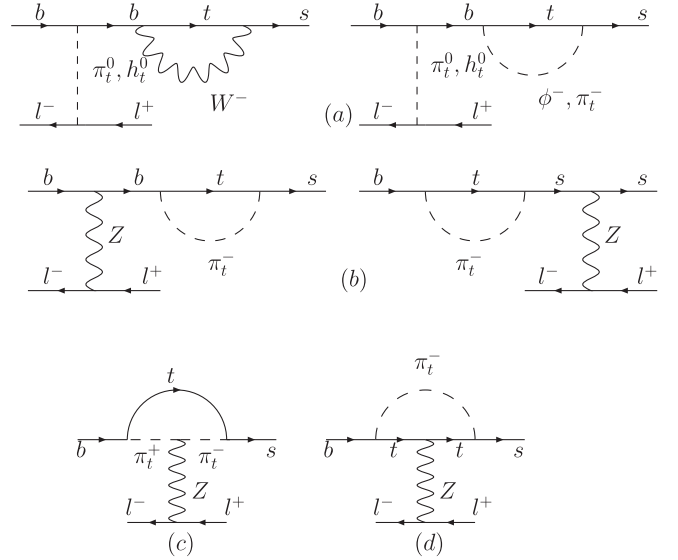


FIG. 3. Scalar particles contributing to $B_s \rightarrow l^+ l^-$ in the $TC2$ model.

The charged top-pions π_t^\pm give contributions to the SM function $Y(x)$ via the diagrams (b), (c) and (d) in Fig. 3, the expression of the function $Y^{TC}(x_s)$ can be written as:

$$Y^{TC}(x_s) = \frac{1}{4\sqrt{2} G_F F_\pi^2} \left[-\frac{x_s^3}{8(1-x_s)} - \frac{x_s^3}{8(1-x_s)^2} \ln x_s \right]. \quad (16)$$

C. Numerical results

The branching ratios of the decay processes $B_s \rightarrow l^+ l^-$ can be written as [3]:

$$\text{Br}(B_s \rightarrow l^+ l^-) = a_s \left[\left| 2m_l R_A - \frac{m_{B_s}^2}{m_b + m_s} R_P \right|^2 + \left(1 - \frac{4m_l^2}{m_{B_s}^2} \right) \left| \frac{m_{B_s}^2}{m_b + m_s} R_S \right|^2 \right], \quad (17)$$

where

$$a_s \equiv \frac{G_F^2 \alpha^2}{64\pi^3} |V_{ts}^* V_{tb}|^2 \tau_{B_s} f_{B_s}^2 m_{B_s} \sqrt{1 - \frac{4m_l^2}{m_{B_s}^2}}. \quad (18)$$

Here τ_{B_s} is the lifetime of B_s .

The longitudinal polarization asymmetry of the final leptons in $B_s \rightarrow l^+ l^-$ is defined as follows [3]:

$$A_{\text{LP}}^\pm \equiv \frac{[\Gamma(s_{l^-}, s_{l^+}) + \Gamma(\mp s_{l^-}, \pm s_{l^+})] - [\Gamma(\pm s_{l^-}, \mp s_{l^+}) + \Gamma(-s_{l^-}, -s_{l^+})]}{[\Gamma(s_{l^-}, s_{l^+}) + \Gamma(\mp s_{l^-}, \pm s_{l^+})] + [\Gamma(\pm s_{l^-}, \mp s_{l^+}) + \Gamma(-s_{l^-}, -s_{l^+})]}, \quad (19)$$

s_{l^\pm} are defined into one direction in dilepton rest frame as $(0, \pm \frac{p_-}{|p_-|})$. For only one direction, there are no differences between the final leptons, thus there is $A_{\text{LP}}^+ = A_{\text{LP}}^- \equiv A_{\text{LP}}$. Then the A_{LP} can be written as:

$$A_{\text{LP}}(B_s \rightarrow l^+ l^-) = \frac{2\sqrt{1 - \frac{4m_l^2}{m_b^2}} \operatorname{Re}\left[\frac{m_{B_s}^2}{m_b + m_s} R_S (2m_l R_A - \frac{m_{B_s}^2}{m_b + m_s} R_P)\right]}{\left|2m_l R_A - \frac{m_{B_s}^2}{m_b + m_s} R_P\right|^2 + \left(1 - \frac{4m_l^2}{m_b^2}\right) \left|\frac{m_{B_s}^2}{m_b + m_s} R_S\right|^2}. \quad (20)$$

$A_{\text{LP}}^{\text{SM}}(B_s \rightarrow l^+ l^-) \simeq 0$ because $R_S \sim \mathcal{O}(10^{-5})$ in the SM.

Before giving numerical results, we need to specify the relevant SM parameters. These parameters have mainly been shown in Table I. We take the coupling constant K_1 , the model dependent parameter ε , the mass of nonuniversal gauge boson $M_{Z'}$ and the mass of scalars M_S as free parameters in our numerical estimation. The value of M_S remains subject to large uncertainty [20]. However, it has been shown that its value is generally allowed to be in the range of a few hundred GeV depending on the models [31]. In our numerical estimation, we will assume that M_S is in the range of 200 GeV \sim 500 GeV. The lower bounds on $M_{Z'}$ can be obtained from dijet and dilepton production in the Tevatron experiments [32] or $B\bar{B}$ mixing [33]. However, these bounds are significantly weaker than those from the precision electroweak data. Reference [34] has

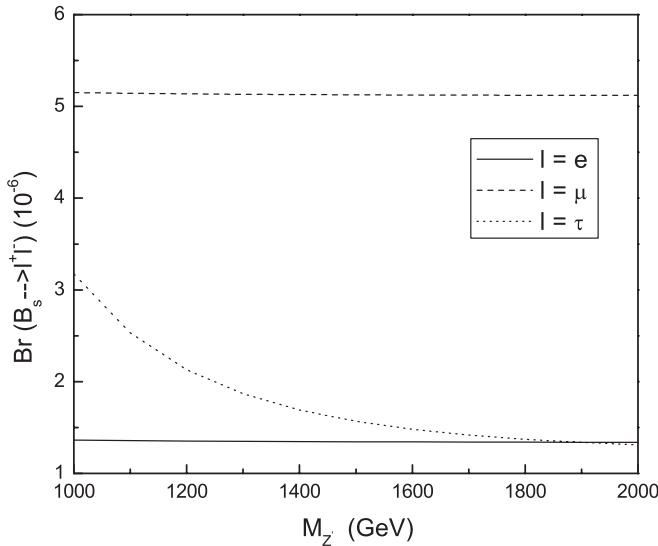
TABLE I. Numerical inputs used in our analysis. Unless explicitly specified, they are taken from the Particle Data Group [29].

$G_F = 1.166 \times 10^{-5} \text{ GeV}^{-2}$	$m_{B_s} = 5.366 \text{ GeV}$
$\alpha = 7.297 \times 10^{-3}$	$m_B = 5.279 \text{ GeV}$
$\tau_{B_s} = (1.437^{+0.031}_{-0.030}) \times 10^{-12} \text{ s}$	$V_{tb} = 1.0$
$\tau_{B_d} = 1.53 \times 10^{-12} \text{ s}$	$V_{ts} = (40.6 \pm 2.7) \times 10^{-3}$
$m_\mu = 0.105 \text{ GeV}$	$f_{B_s} = (0.259 \pm 0.027) \text{ GeV}$ [30]
$M_W = 80.425(38) \text{ GeV}$	$\sin^2 \theta_W = 0.23120(15)$

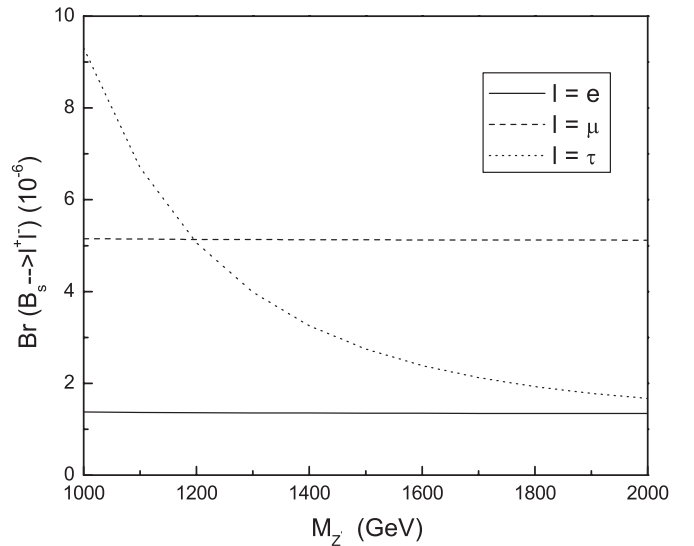
shown that, to fit the precision electroweak data, the Z' mass $M_{Z'}$ must be larger than 1 TeV. In our numerical estimation, we will assume that the values of the free parameters ε , K_1 and $M_{Z'}$ are in the range of 0.03 \sim 0.1, 0 \sim 1 and 1000 GeV \sim 2000 GeV, respectively.

First we give our numerical results of the decay processes $B_s \rightarrow l^+ l^-$ induced by the nonuniversal gauge boson Z' . The branching ratios of $B_s \rightarrow l^+ l^-$ are plotted in Fig. 4 as function of the mass parameter $M_{Z'}$ for $K_1 = 0.4$ and 0.8, in which we have multiplied the factors 10^7 and 10^3 to the values of $\text{Br}(B_s \rightarrow e^+ e^-)$ and $\text{Br}(B_s \rightarrow \mu^+ \mu^-)$, respectively. From these figures one can see that the values of $\text{Br}(B_s \rightarrow \tau^+ \tau^-)$ are sensitive to the mass of Z' , they increase as the mass parameter $M_{Z'}$ decreasing. For $l = e, \mu$, the values of their branching ratios are not so sensitive to the parameter $M_{Z'}$. Because the contributions of Z' to $\text{Br}(B_s \rightarrow e^+ e^-)$ and $\text{Br}(B_s \rightarrow \mu^+ \mu^-)$ are small relative to the SM contributions. The values of the corresponding branching ratios are both below $\mathcal{O}(10^{-9})$ which are not easy to be observed in current collider experiments. The contributions of Z' to the branching ratio of the decay $B_s \rightarrow \tau^+ \tau^-$ are large, since the nonuniversal gauge boson Z' has large couplings to the third generation fermion with respect to the first two generations, it can make the branching ratio value reach $\mathcal{O}(10^{-6})$ with reasonable values of the free parameters.

The branching ratios of $B_s \rightarrow l^+ l^-$ contributed by the scalars ($\pi_i^{0,\pm}$ and h_i^0) are plotted in Fig. 5 as function of the



(a) $K_1 = 0.4$



(b) $K_1 = 0.8$

FIG. 4. The branching ratios of $B_s \rightarrow l^+ l^-$ as function of the parameter $M_{Z'}$ for $K_1 = 0.4$ (a) and $K_1 = 0.8$ (b).

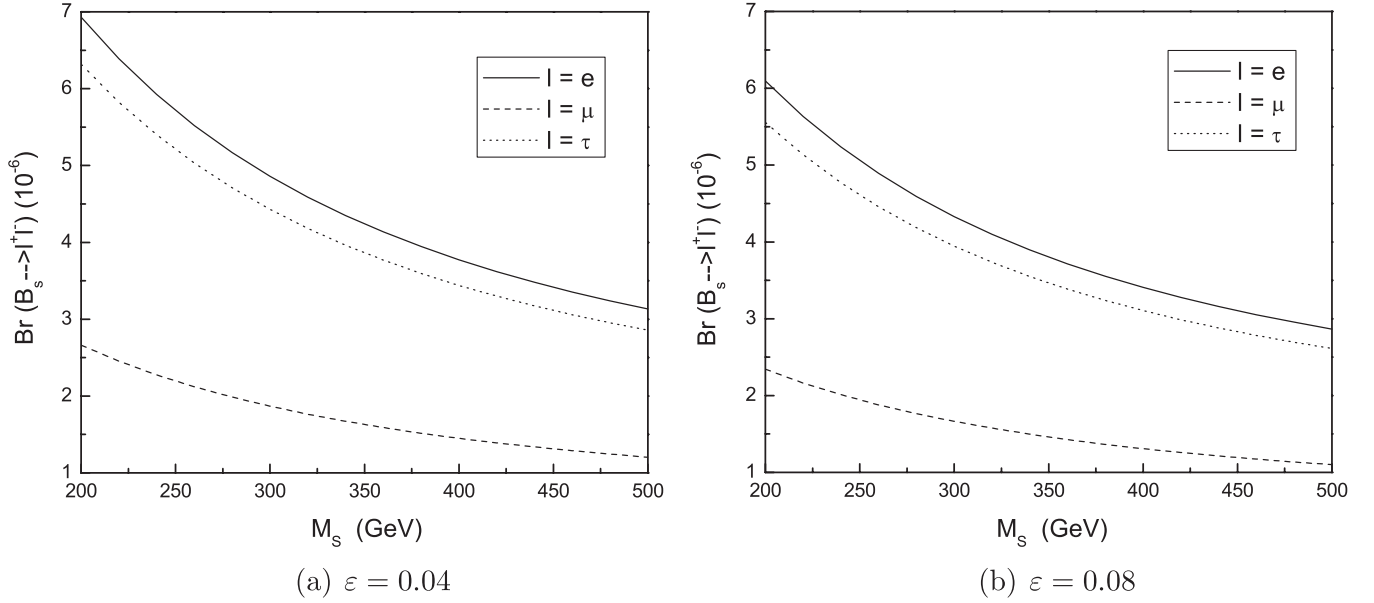


FIG. 5. The branching ratios of $B_s \rightarrow l^+ l^-$ as function of the parameter M_S for $\varepsilon = 0.04$ (a) and $\varepsilon = 0.08$ (b).

mass parameter M_S for $\varepsilon = 0.04$ and 0.08 , in which we have multiplied the factors 10^7 and 10^2 to the values of $\text{Br}(B_s \rightarrow e^+ e^-)$ and $\text{Br}(B_s \rightarrow \mu^+ \mu^-)$, respectively. It is obvious that the values of the branching ratios for these decays increase as the parameter M_S decreasing. Furthermore, the enhancement to the branching ratio of the decay process $B_s \rightarrow \mu^+ \mu^-$ is larger than that of the Z' contributions by an order of magnitude.

The value of $\text{Br}(B_s \rightarrow e^+ e^-)$ is smaller than that of $\text{Br}(B_s \rightarrow \mu^+ \mu^-)$ by five orders of magnitude, which is because it is suppressed by m_e^2/m_μ^2 with respect to μ channel. The branching ratio for $\tau^+ \tau^-$ mode is enhanced

by a factor of 10^2 to μ channel, its value can reach $\mathcal{O}(10^{-6})$ by our calculation. However, the $\tau^+ \tau^-$ channel is still not easy to be observed under present experimental precision, while the current experimental upper limit for $\text{Br}(B_s \rightarrow \tau^+ \tau^-)$ from the BABAR collaboration is 4.1×10^{-3} at 90% C.L. [35]. So the experimental searches for $B_s \rightarrow l^+ l^-$ have focused on the μ channel, and we only discuss this channel. Comparing with the SM prediction $\text{Br}(B_s \rightarrow \mu^+ \mu^-) = 3.86 \pm 0.15 \times 10^{-9}$ [1], the contributions of the new scalars predicted by the $TC2$ model can enhance this value by one order of magnitude, so our results are more approach to the experimental data given by Eq. (1).

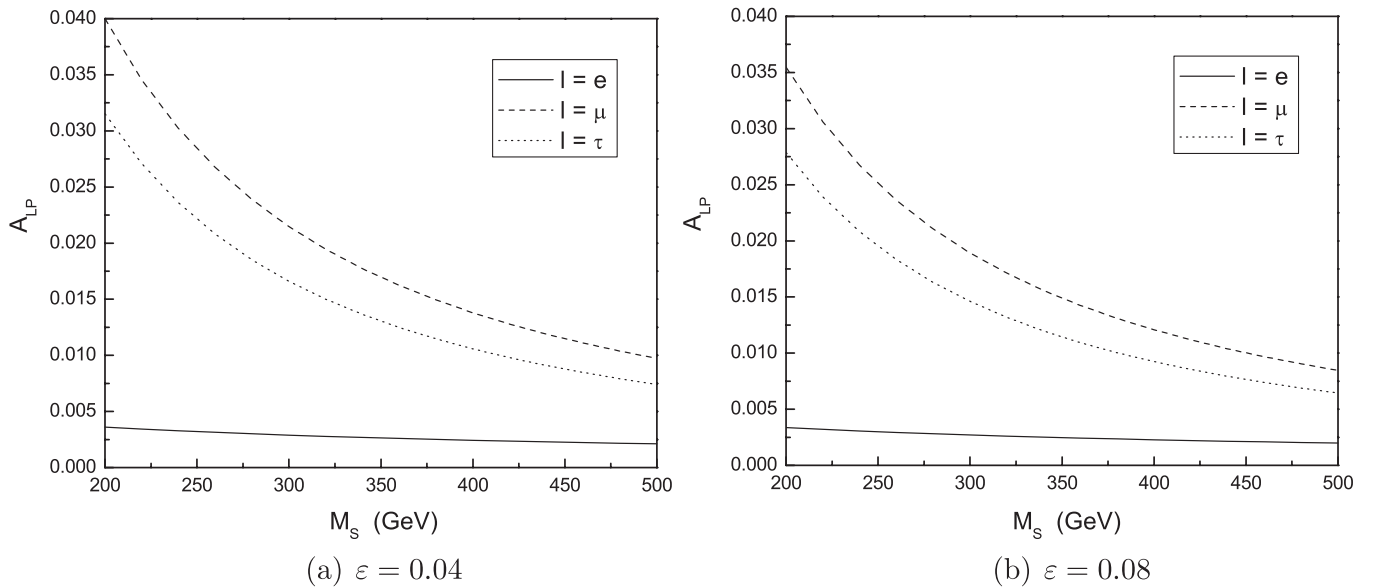


FIG. 6. The longitudinal polarization asymmetry in $B_s \rightarrow l^+ l^-$ as function of the parameter M_S for $\varepsilon = 0.04$ (a) and $\varepsilon = 0.08$ (b).

Obviously, the nonuniversal gauge boson Z' has no contributions to the SPNP operators, so it was not considered in this subsection. The longitudinal polarization asymmetry A_{LP} contributed by the new scalars predicted by the $TC2$ model as function of the parameter M_S are plotted in Fig. 6. From these figures one can see that the A_{LP} is sensitive to the mass of the scalars, especially for $l = \mu, \tau$, however it is less sensitive to the parameter ε . The values of the asymmetry A_{LP} can reach nearly 4% for $l = \mu, \tau$ when the mass of the scalars get to 200 GeV.

IV. THE CONTRIBUTIONS OF THE $TC2$ MODEL TO THE RARE DECAY PROCESSES $B \rightarrow Kl^+l^-$

The effective Hamilton for the decay $B \rightarrow Kl^+l^-$ is similar to that of $B_s \rightarrow l^+l^-$ as shown in Eq. (9), which is constituted by two parts. The SPNP part is same as the expression shown in Eq. (11). In the framework of the $TC2$ model, The H_0 part can be written as [27]:

$$H_0 = \frac{\alpha G_F}{\sqrt{2}\pi} V_{tb} V_{ts}^* \{ C_9^{\text{eff}} (\bar{s} \gamma_\mu P_L b) \bar{l} \gamma_\mu l + C_{10} (\bar{s} \gamma_\mu P_L b) \bar{l} \gamma_\mu \gamma_5 l - 2 \frac{C_7^{\text{eff}}}{q^2} m_b (\bar{s} i \sigma_{\mu\nu} q^\nu P_R b) \bar{l} \gamma_\mu l \}. \quad (21)$$

Here q_μ is the sum of 4-momenta of l^+ and l^- . The Wilson coefficients C_7^{eff} , C_9^{eff} and C_{10} contain two parts of contributions from the SM and the $TC2$ model.

Similar to the decay processes $B_s \rightarrow l^+l^-$, the nonuniversal gauge boson Z' give contributions to the Wilson coefficients C_9^{eff} and C_{10} , the relevant Feynman diagrams are same as Fig. 1 and the relevant functions $Y^{TC}(x_t)$ and $Z^{TC}(x_t)$ have same expressions as shown in Eq. (12).

The charged top-pions π_t^\pm can give contributions to the Wilson coefficients C_7^{eff} and C_9^{eff} . The relevant Feynman diagrams are similar to Fig. 3. However, these penguin diagrams are induced by γ penguins, gluon penguins, and chromomagnetic penguins. The coefficients C_7^{eff} and C_9^{eff} can be expressed in terms of the corresponding functions $D_1(x_s)$, $E_1(x_s)$, and $E'_1(x_s)$, which are added to the corresponding SM functions $D_0(x_t)$, $E_0(x_t)$ and $E'_0(x_t)$ [28]. The detailed expression forms of the these functions are [36]:

$$D_1(x) = \frac{1}{4\sqrt{2}G_F F_\pi} \left(\frac{47 - 79x + 38x^2}{108(1-x)^3} + \frac{3 - 6x^2 + 4x^3}{18(1-x)^4} \ln(x) \right), \quad (22)$$

$$E_1(x) = \frac{1}{4\sqrt{2}G_F F_\pi} \left(\frac{7 - 29x + 16x^2}{36(1-x)^3} - \frac{3x^2 - 2x^3}{6(1-x)^4} \ln(x) \right), \quad (23)$$

$$E'_1(x) = \frac{1}{8\sqrt{2}G_F F_\pi} \left(\frac{5 - 19x + 20x^2}{6(1-x)^3} - \frac{x^2 - 2x^3}{(1-x)^4} \ln(x) \right). \quad (24)$$

We can obtain the corrected Wilson coefficients C_7^{eff} , C_9^{eff} and C_{10} with these corrected functions using the relevant expressions of these coefficients in Refs. [10,36], which are listed in Appendix C. The neutral top-pion π_t^0 and top-Higgs h_t^0 can also give contributions to these decay processes through the SPNP operators, and the expression forms of R_S (R_P) are same as those shown in Eq. (15).

The branching ratios $\text{Br}(B \rightarrow Kl^+l^-)$ ($l = e, \mu$ and τ) contributed by the gauge boson Z' are plotted in Fig. 7 as a function of the mass parameter $M_{Z'}$ for two values of K_1 , in which we have multiplied the factor 10^{-1} and 10^{-2} to the branching ratios of decays $B \rightarrow K\mu^+\mu^-$ and $B \rightarrow K\tau^+\tau^-$ respectively. From this figure one can see that the values of the branching ratios for $l = e, \mu$, and τ increase as the parameter $M_{Z'}$ is decreasing. However, the branching ratios for $l = e$ are not sensitive to the parameter $M_{Z'}$ as shown in these figures. The values of the branching ratios for $l = e$ and μ are not sensitive to the parameter K_1 . For $K_1 = 0.4$ and $1000 \text{ GeV} \leq M_{Z'} \leq 2000 \text{ GeV}$, the values of $\text{Br}(B \rightarrow Ke^+e^-)$ and $\text{Br}(B \rightarrow K\mu^+\mu^-)$ are in the range of $6.1 \times 10^{-8} \sim 4.4 \times 10^{-8}$ and $3.0 \times 10^{-7} \sim 1.2 \times 10^{-7}$, respectively.

The branching ratios of the decay processes $B \rightarrow Kl^+l^-$ contributed by the scalars ($\pi_t^{0,\pm}, h_t^0$) are plotted in Fig. 8 as function of the mass parameter M_S for $\varepsilon = 0.04$ and 0.08 , in which we have multiplied the factors 10^{-1} to the branching ratio of $B \rightarrow K\mu^+\mu^-$. From these figures, one can see that the values of the branching ratios of these decay processes increase as the parameter M_S decreasing. All of their values are not sensitive to the parameter ε . The contributions of the scalars for $l = e$ and μ are comparable to those of the nonuniversal gauge boson Z' , the values of the branching ratios of $B \rightarrow Ke^+e^-$ and $B \rightarrow K\mu^+\mu^-$ contributed by both the scalars and the nonuniversal gauge boson can reach $\mathcal{O}(10^{-7})$, which give an explanation to the deviation between the experimental data and the SM predictions in Ref. [8]. While the scalar's contribution to the decay process $B \rightarrow K\tau^+\tau^-$ is smaller than that of the nonuniversal gauge boson Z' by two order of magnitude and therefore can be neglected. When the Z' mass is in the range of $1000 \text{ GeV} \sim 2000 \text{ GeV}$, the values of $\text{Br}(B \rightarrow K\tau^+\tau^-)$ are in the range of $7.0 \times 10^{-6} \sim 1.7 \times 10^{-6}$. This result is 2 orders of magnitude larger than the e and μ channel, which is because of the large coupling of Z' to the third-generation fermions.

The normalized forward-backward (FB) asymmetry can be defined as [4]:

$$A_{\text{FB}}(z) = \frac{\int_0^1 d \cos \theta \frac{d^2 \Gamma}{dz d \cos \theta} - \int_{-1}^0 d \cos \theta \frac{d^2 \Gamma}{dz d \cos \theta}}{\int_0^1 d \cos \theta \frac{d^2 \Gamma}{dz d \cos \theta} + \int_{-1}^0 d \cos \theta \frac{d^2 \Gamma}{dz d \cos \theta}}. \quad (25)$$

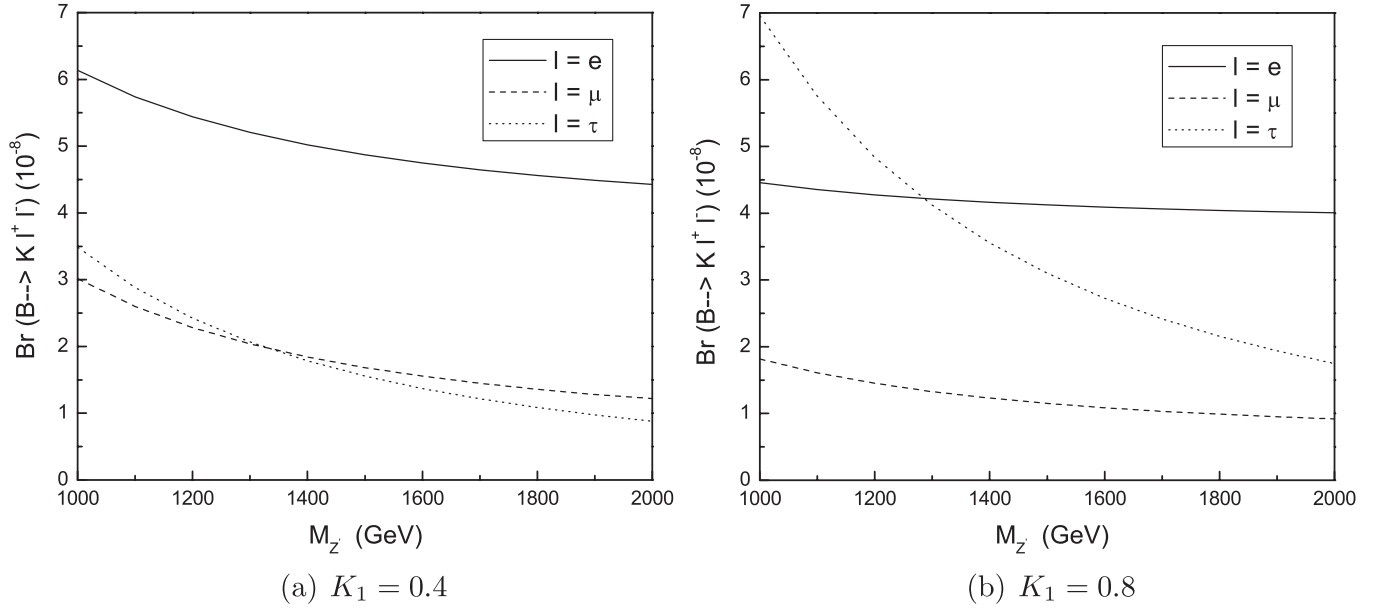


FIG. 7. The branching ratios of $B \rightarrow Kl^+l^-$ as function of the parameter M_Z for $K_1 = 0.4$ (a) and $K_1 = 0.8$ (b).

After the integral calculation of FB asymmetry gives,

$$\langle A_{\text{FB}} \rangle = \frac{2\tau_B \Gamma_0 \hat{m}_l \beta_\mu^2 R_S \int dz a_1(z) \phi(1, k^2, z)}{\text{Br}(B \rightarrow Kl^+l^-)}, \quad (26)$$

where τ_B is the lifetime of B meson and $\text{Br}(B \rightarrow Kl^+l^-)$ is the total branching ratio of $B \rightarrow Kl^+l^-$ and Γ_0 is the total width of the B meson, which can be written as:

$$\Gamma_0 = \frac{G_F^2 \alpha^2}{2^9 \pi^5} |V_{tb} V_{ts}^*|^2 m_B^5, \quad (27)$$

$$a_1(z) = \frac{1}{2} (1 - k^2) C_9 f_0(z) f_+(z) + (1 - k) C_7 f_0(z) f_T(z). \quad (28)$$

Other relevant functions such as $\phi(1, k^2, z)$ are listed in Appendix C. The form factors f_+ , f_0 , and f_T are defined in the relevant matrix elements as:

$$\begin{aligned} \langle K(p') | \bar{s} \gamma_\mu b | B(p) \rangle &= (2p - q)_\mu f_+(z) \\ &+ \left(\frac{1 - k^2}{z} \right) q_\mu [f_0(z) - f_+(z)], \end{aligned} \quad (29)$$

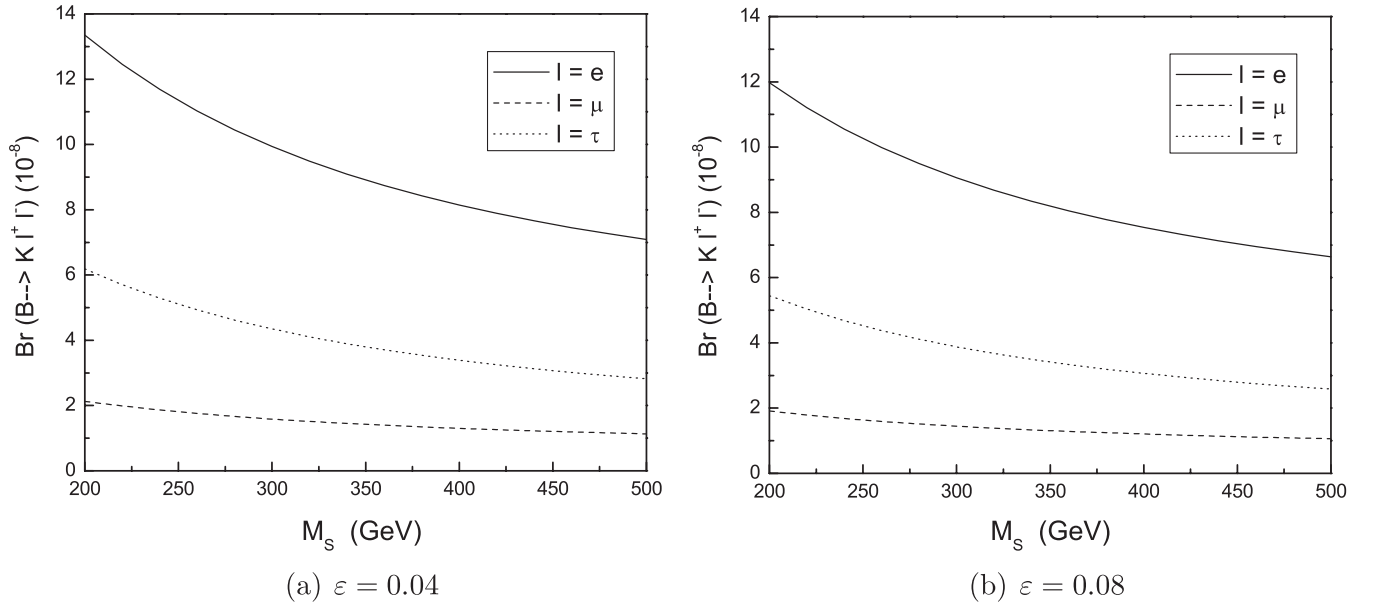


FIG. 8. The branching ratios of $B \rightarrow Kl^+l^-$ as function of the parameter M_S for $\varepsilon = 0.04$ (a) and $\varepsilon = 0.08$ (b).

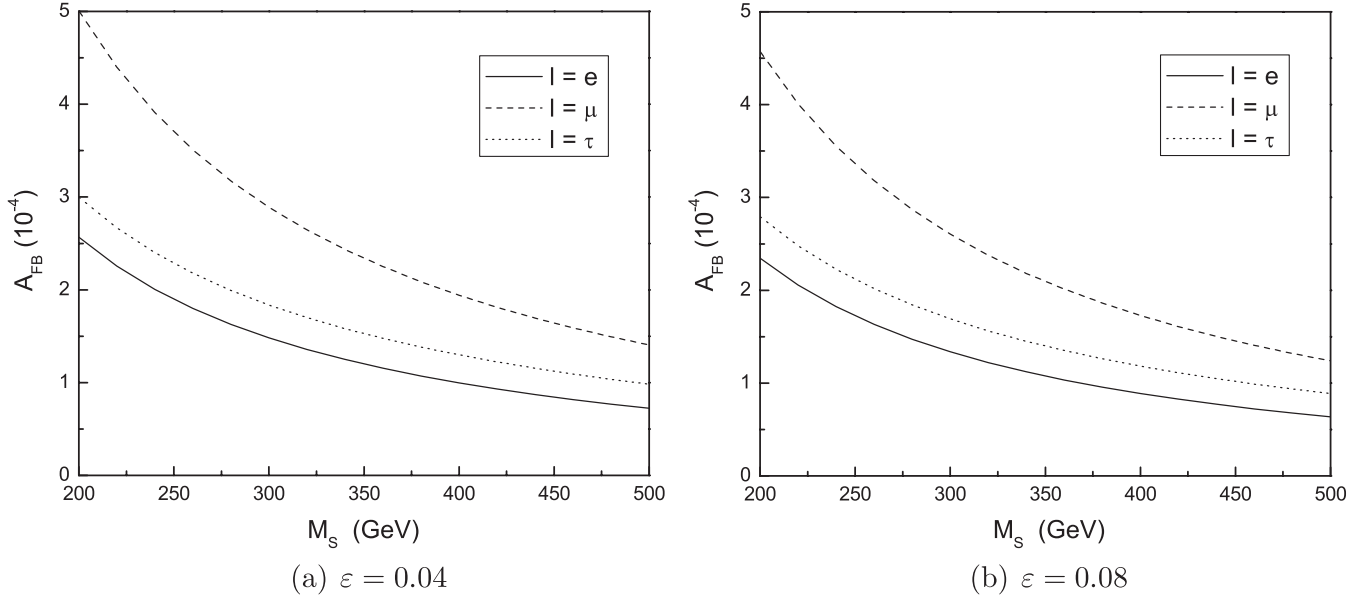


FIG. 9. In the $TC2$ model, the forward-backward asymmetry in $B \rightarrow Kl^+l^-$ as function of M_S for the parameter $\varepsilon = 0.04$ (a) and $\varepsilon = 0.08$ (b).

$$\begin{aligned} \langle K(p') | \bar{s} i \sigma_{\mu\nu} q^\nu b | B(p) \rangle = & -[(2p - q)_\mu q^2 \\ & - (m_B^2 - m_K^2) q_\mu] \frac{f_T(z)}{m_B + m_K}, \end{aligned} \quad (30)$$

$$\langle K(p') | \bar{s} b | B(p) \rangle = \frac{m_B(1 - k^2)}{\hat{m}_b} f_0(z). \quad (31)$$

Here, $k \equiv m_K/m_B$, $z \equiv q^2/m_B^2$, and $\hat{m}_b \equiv m_b/m_B$. The form factors f_+ , f_0 , and f_T can be calculated by using the light cone QCD approach. Their particular forms can be found in Ref. [27]. In this paper, we assume $\hat{m}_b \approx 1$.

The production of the FB asymmetries are only sensitive to SPNP operators. From Eq. (26), one can see that the nonuniversal gauge boson Z' has no contribution to the FB asymmetry, so we only discuss the contributions coming from the scalars ($\pi_i^{0,\pm}$, h_i^0).

The FB asymmetry A_{FB} of leptons in the decay processes $B \rightarrow Kl^+l^-$ are plotted in Fig. 9 as function of the parameter M_S for $\varepsilon = 0.04$ and 0.08 , in which we have multiplied the factors 10^5 and 10 to the value of $A_{FB}(B \rightarrow Ke^+e^-)$ and $A_{FB}(B \rightarrow K\mu^+\mu^-)$ respectively. From this figure one can see that the value of A_{FB} is smaller than $\mathcal{O}(10^{-3})$ in most of the parameter spaces. Comparing its experimental measurement value, this value is not large enough to be observed in experiments. One can see that the contributions of the $TC2$ model to the FB asymmetry in these decay processes are smaller than those of the SUSY models. Considering the uncertainty in measurements, it is very difficult to detect the signals of the $TC2$ model through measuring the FB asymmetry about these decay processes.

V. THE CONTRIBUTIONS OF THE LHT MODEL TO THE RARE DECAY PROCESSES $b \rightarrow sl^+l^-$

The LHT model [14] is based on an $SU(5)/SO(5)$ global symmetry breaking pattern. A subgroup $[SU(2) \times U(1)]_1 \times [SU(2) \times U(1)]_2$ of the $SU(5)$ global symmetry is gauged, and at the scale f it is broken into the SM electroweak symmetry $SU(2)_L \times U(1)_Y$. T-parity is an automorphism which exchanges the $[SU(2) \times U(1)]_1$ and $[SU(2) \times U(1)]_2$ gauge symmetries. The T-even combinations of the gauge fields are the SM electroweak gauge bosons W_μ^a and B_μ . The T-odd combinations are T-parity partners of the SM electroweak gauge bosons.

After taking into account EWSB, at the order of v^2/f^2 , the masses of the T-odd set of the $SU(2) \times U(1)$ gauge bosons are given as:

$$\begin{aligned} M_{B_H} &= \frac{g' f}{\sqrt{5}} \left[1 - \frac{5\nu^2}{8f^2} \right], \\ M_{Z_H} &\approx M_{W_H} = g f \left[1 - \frac{\nu^2}{8f^2} \right], \end{aligned} \quad (32)$$

where f is the scale parameter of the gauge symmetry breaking of the LHT model. g' is the SM $U(1)_Y$ gauge coupling constants. Because of the smallness of g' , the T-odd gauge boson B_H is the lightest T-odd particle, which can be seen as an attractive dark matter candidate [37]. To avoid severe constraints and simultaneously implement T-parity, it is necessary to double the SM fermion doublet spectrum [14,38]. The T-even combination is associated with the $SU(2)_L$ doublet, while the T-odd combination is its T-parity partner. The masses of the T-odd fermions can be written in a unified manner as:

$$M_{F_i} = \sqrt{2}k_i f, \quad (33)$$

where k_i are the eigenvalues of the mass matrix k and their values are generally dependent on the fermion species i .

The mirror fermions (T-odd quarks and T-odd leptons) have new flavor violating interactions with the SM fermions mediated by the new gauge bosons (B_H , W_H^\pm , or Z_H), which are parametrized by four CKM-like unitary mixing matrices, two for mirror quarks and two for mirror leptons [39,40]:

$$V_{Hu}, \quad V_{Hd}, \quad V_{Hl}, \quad V_{H\nu}. \quad (34)$$

They satisfy:

$$V_{Hu}^\dagger V_{Hd} = V_{\text{CKM}}, \quad V_{H\nu}^\dagger V_{Hl} = V_{\text{PMNS}}. \quad (35)$$

Where the CKM matrix V_{CKM} is defined through flavor mixing in the down-type quark sector, while the PMNS matrix V_{PMNS} is defined through neutrino mixing.

The contributions of the LHT model to the rare decay processes $b \rightarrow s l^+ l^-$ are mainly coming from the corrections to the Wilson coefficients, which related to the SM Inami-Lim functions [28]. The branching ratios of the decay processes $B_s \rightarrow l^+ l^-$ in the SM depend on a function Y_{SM} and the LHT effects enter through the modification of the function Y_{SM} [39]. With the LHT effects Y_{SM} is replaced by [15]:

$$Y_s = Y_{\text{SM}} + \bar{Y}^{\text{even}} + \frac{\bar{Y}_s^{\text{odd}}}{\lambda_t^{(s)}}, \quad (36)$$

where \bar{Y}^{even} and \bar{Y}_s^{odd} represent the effects from T-even and T-odd particles, respectively. The branching ratios normalized to the SM predictions are then given by:

$$\frac{\text{Br}(B_s \rightarrow l^+ l^-)}{\text{Br}(B_s \rightarrow l^+ l^-)_{\text{SM}}} = \left| \frac{Y_s}{Y_{\text{SM}}} \right|^2, \quad (37)$$

which $\text{Br}(B_s \rightarrow l^+ l^-)_{\text{SM}}$ are the branching ratios predicted by the SM. Their particular numerical values of the branching ratios for the decay processes $B_s \rightarrow l^+ l^-$ in the LHT model are listed as follows:

$$\text{Br}(B_s \rightarrow e^+ e^-) = (1.36 \pm 0.05) \times 10^{-13}, \quad (38)$$

$$\text{Br}(B_s \rightarrow \mu^+ \mu^-) = (5.79 \pm 0.23) \times 10^{-9}, \quad (39)$$

$$\text{Br}(B_s \rightarrow \tau^+ \tau^-) = (1.23 \pm 0.05) \times 10^{-6}. \quad (40)$$

The branching ratios of the decay processes $B \rightarrow Kl^+ l^-$ in the SM depend on the functions Y_{SM} , Z_{SM} and $D'_0(x_t)$ ($D'_0(x_t)$ is same as in $B \rightarrow X_s \gamma$ [15]), the LHT effects enter through the modification of these functions. The modifications of the function Y_{SM} has been given above, and the modifications of the function Z_{SM} is given by [15,39]:

$$Z_s = Z_{\text{SM}} + \bar{Z}^{\text{even}} + \frac{\bar{Z}_s^{\text{odd}}}{\lambda_t^{(s)}}, \quad (41)$$

where \bar{Z}^{even} and \bar{Z}_s^{odd} represent the effects coming from T-even and T-odd particles, respectively. Similar with Sec. IV, we can calculate the contributions of the LHT model to the decay processes $B \rightarrow Kl^+ l^-$. With reasonable values of the free parameters in the framework of the LHT model, the maximum values of the branching ratios for the rare decays $B \rightarrow Kl^+ l^-$ are:

$$\text{Br}(B \rightarrow Ke^+ e^-) = 9.66 \times 10^{-6}, \quad (42)$$

$$\text{Br}(B \rightarrow K\mu^+ \mu^-) = 6.56 \times 10^{-6}, \quad (43)$$

$$\text{Br}(B \rightarrow K\tau^+ \tau^-) = 2.99 \times 10^{-7}. \quad (44)$$

These numerical results are obtained by calculating the relative correction to the SM predictions in the framework of the LHT model, while the SM predictions exist the uncertainty coming from the next-to-leading logarithmic (NLO) contributions and the long-distance contributions, for which the $\text{Br}(B \rightarrow Kl^+ l^-)$ are a little disparity away from their respective experimental upper limits [41]. However, there is no disagreement with experiment in some parameter ranges while the corrected effects is no more than 15%.

The contributions of the LHT model to the asymmetry observables A_{FB} and A_{LP} in the rare decay processes $b \rightarrow s l^+ l^-$ mainly come from the new neutral scalar particles. For the B_s meson, there is an unitarity relation of the V_{Hd} matrix [39]:

$$\xi_1^{(s)} + \xi_2^{(s)} + \xi_3^{(s)} = 0, \quad (45)$$

where $\xi_i^{(s)} = V_{Hd}^{*ib} V_{Hd}^{is}$. Considering this relation, the calculations of the relevant Feynman diagrams similar to Fig. 3 equal to zero. Hence, in the framework of the LHT model, the total contributions induced by the neutral scalars are equal to zero. The contributions to the A_{FB} and A_{LP} is close to the predictions in the SM.

VI. CONCLUSIONS

The SM is a very successful theory but it can only be an effective theory below some high energy scales. To completely avoid the problems arising from the elementary Higgs field in the SM various kinds of dynamical electro-weak symmetry breaking models have been proposed, among which the topcolor scenario is attractive because it can explain the large top quark mass and provide a possible EWSB mechanism. The $TC2$ model has all essential features of the topcolor scenario. It is expected that the possible signals of the $TC2$ model should be detected in the future high energy collider experiments.

In this paper we consider the contributions of the $TC2$ model to observables related to the decay processes $B_s \rightarrow l^+ l^-$ and $B \rightarrow Kl^+ l^-$. We find that the $TC2$ model can enhance the branching ratios of the SM predictions for these decay processes $B_s \rightarrow l^+ l^-$ and $B \rightarrow Kl^+ l^-$. In wide ranges of the free parameter space, it is possible to enhance the values of $\text{Br}(B_s \rightarrow l^+ l^-)$ and $\text{Br}(B \rightarrow Kl^+ l^-)$ by one order of magnitude. In the $TC2$ model, the nonuniversal gauge boson Z' gives main contributions to $\text{Br}(B_s \rightarrow \tau^+ \tau^-)$, while the contributions of Z' to $\text{Br}(B_s \rightarrow e^+ e^-)$ and $\text{Br}(B_s \rightarrow \mu^+ \mu^-)$ are comparable with those of the new scalars ($\pi_i^{0,\pm}, h_i^0$). For the decay processes $B \rightarrow Ke^+ e^-$ and $B \rightarrow K\mu^+ \mu^-$, the contributions of Z' are comparable with those of the scalars. While the contributions of the $TC2$ model to $\text{Br}(B \rightarrow K\tau^+ \tau^-)$ mainly come from Z' .

The production of the asymmetries are only sensitive to SPNP operators, so there are no contributions of Z' to the relevant observables. We further calculate the contributions of the new scalars predicted by the $TC2$ model to the asymmetry observables A_{FB} and A_{LP} of leptons in the decay processes $B_s \rightarrow l^+ l^-$ and $B \rightarrow Kl^+ l^-$. Our numerical results show that, when the mass of the scalars gets to 200 GeV, the values of the asymmetry A_{LP} in the decay processes $B_s \rightarrow \mu^+ \mu^-$ and $B_s \rightarrow \tau^+ \tau^-$ can reach 4%. We hope that the values of A_{LP} for $l = \mu, \tau$ can approach the detectability threshold of the near future experiments. However, the contributions of these new scalars to A_{FB} are around $\mathcal{O}(10^{-4})$ in most of the parameter space, which are not large enough to be detected.

The LHT model is one of the attractive little Higgs models, which satisfies the electroweak precision data in most of the parameter space. This model can produce rich phenomenology at present and in future high energy experiments. New particles predicted by this model give contributions to the branching ratios of the rare decay processes $B_s \rightarrow l^+ l^-$ and $B \rightarrow Kl^+ l^-$. Reference [15] has shown that, comparing with their SM predictions, the branching ratios of the decay processes $B_s \rightarrow l^+ l^-$ and $B \rightarrow Kl^+ l^-$ can be enhanced by at most 50% and 15%, respectively. For comparison, we give a brief description and particular numerical results about these rare decays. In addition, we show that the neutral scalars predicted by this model can not give contributions to the asymmetry observables A_{FB} and A_{LP} .

In conclusion, the effects of the $TC2$ model on the branching ratios and asymmetry observables related to the rare decay processes $b \rightarrow s l^+ l^-$ can give positive contributions to the SM predictions. The numerical results show that the branching ratios for these decays are much close to the experimental data, such as $\text{Br}(B_s \rightarrow \mu^+ \mu^-)$. The value of $\text{Br}(B \rightarrow K\tau^+ \tau^-)$ is larger than the SM prediction by one order of magnitude, which is hoped to be observed in the future high accuracy experiments, or the future experimental results may give constraints on the free

parameters of the $TC2$ model. Hence, it is indicated that the possible signals of the $TC2$ model may be observed through the above decay processes in future experiments.

ACKNOWLEDGMENTS

This work was supported in part by the National Natural Science Foundation of China under Grants No. 10675057, Specialized Research Fund for the Doctoral Program of Higher Education (SRFDP) (No. 200801650002), the Natural Science Foundation of the Liaoning Scientific Committee (No. 20082148), and Foundation of Liaoning Educational Committee (No. 2007T086).

APPENDIX A: RELEVANT FUNCTIONS IN THE SM

In this Appendix we list the functions in the SM that entered the present study of rare B decays.

$$Y^{\text{SM}}(x) = \frac{1}{8} \left[\frac{x-4}{x-1} + \frac{3x}{(x-1)^2} \log x \right], \quad (\text{A1})$$

$$Z^{\text{SM}}(x_l) = -\frac{1}{9} \log x_l + \frac{18x_l^4 - 163x_l^3 + 259x_l^2 - 108x_l}{144(x_l - 1)^3} + \frac{32x_l^4 - 38x_l^3 - 15x_l^2 + 18x_l}{72(x_l - 1)^4} \log x_l, \quad (\text{A2})$$

$$D_0(y) = -\frac{4}{9} \log y + \frac{-19y^3 + 25y^2}{36(y-1)^3} + \frac{y^2(5y^2 - 2y - 6)}{18(y-1)^4} \times \log y, \quad (\text{A3})$$

$$E_0(y) = -\frac{2}{3} \log y + \frac{y^2(15 - 16y + 4y^2)}{6(y-1)^4} \log y + \frac{y(18 - 11y - y^2)}{12(1-y)^3}, \quad (\text{A4})$$

$$D'_0(y) = -\frac{(3y^3 - 2y^2)}{2(y-1)^4} \log y + \frac{(8y^3 + 5y^2 - 7y)}{12(y-1)^3}, \quad (\text{A5})$$

$$E'_0(y) = \frac{3y^2}{2(y-1)^4} \log y + \frac{(y^3 - 5y^2 - 2y)}{4(y-1)^3}. \quad (\text{A6})$$

APPENDIX B: RELEVANT FUNCTIONS IN THE $TC2$ MODEL

In this Appendix we list the functions that entered the present study of rare B decays in the framework of the $TC2$ model.

$$C_{ab}(x) = -\frac{2g^2 c_w^2 F_1(x)}{3g_2^2 (v_d + a_d)}, \quad (\text{B1})$$

$$C_c(x) = \frac{2f^2 c_w^2}{g_2^2} \left(\frac{2F_2(x)}{3(v_u + a_u)} + \frac{F_3(x)}{6(v_u - a_u)} \right), \quad (\text{B2})$$

$$C_d(x) = \frac{2f^2 c_w^2}{g_2^2} \left(\frac{2F_4(x)}{3(v_u + a_u)} + \frac{F_5(x)}{6(v_u - a_u)} \right), \quad (\text{B3})$$

$$C(x) = \frac{F_1(x)}{-(0.5(Q-1)s_w^2 + 0.25)}. \quad (\text{B4})$$

Here the variables are defined as: $g = \sqrt{4\pi K_1}$, $v_{u,d} = I_3 - 2Q_{u,d}s_w^2$, $s_w = \sin\theta_w$, $a_{u,d} = I_3$, where u, d represent the up and down-type quarks, respectively.

$$F_1(x) = -(0.5(Q-1)s_w^2 + 0.25)(x^2 \ln(x)/(x-1)^2 - x/(x-1) - x(0.5(-0.5772 + \ln(4\pi)) - \ln(M_W^2)) + 0.75 - 0.5(x^2 \ln(x)/(x-1)^2 - 1/(x-1))), \quad (\text{B5})$$

$$F_2(x) = (0.5Qs_w^2 - 0.25)(x^2 \ln(x)/(x-1)^2 - 2x \ln(x)/(x-1)^2 + x/(x-1)), \quad (\text{B6})$$

$$F_3(x) = -Qs_w^2(x/(x-1) - x \ln(x)/(x-1)^2), \quad (\text{B7})$$

$$F_4(x) = 0.25(4s_w^2/3 - 1)(x^2 \ln(x)/(x-1)^2 - x - x/(x-1)), \quad (\text{B8})$$

$$F_5(x) = -0.25Qs_w^2 x(-0.5772 + \ln(4\pi) - \ln(M_W^2) + 1 - x \ln(x)/(x-1) - s_w^2/6(x^2 \ln(x)/(x-1)^2 - x - x/(x-1))). \quad (\text{B9})$$

APPENDIX C: RELEVANT EXPRESSIONS IN OUR CALCULATION

In this Appendix we list the functions that entered the present study of rare B decays and some expressions of the relevant coefficients.

$$M(B \rightarrow Kl^+l^-) = \frac{\alpha G_F}{2\sqrt{2}\pi} V_{tb} V_{ts}^* \left[\langle K(p') | \bar{s} \gamma_\mu b | B(p) \rangle \{ C_9^{\text{eff}} \bar{u}(p_+) \gamma_\mu v(p_-) + C_{10} \bar{u}(p_+) \gamma_\mu \gamma_5 v(p_-) \} - 2 \frac{C_7^{\text{eff}}}{q^2} m_b \langle K(p') | \bar{s} i \sigma_{\mu\nu} q^\nu b | B(p) \rangle \bar{u}(p_+) \gamma_\mu v(p_-) + \langle K(p') | \bar{s} b | B(p) \rangle \{ R_S \bar{u}(p_+) v(p_-) + R_P \bar{u}(p_+) \gamma_5 v(p_-) \} \right], \quad (\text{C1})$$

$$\frac{d^2\Gamma}{dzd\cos\theta} = \frac{G_F^2 \alpha^2}{2^9 \pi^5} |V_{tb} V_{ts}^*|^2 m_B^5 \phi^{1/2}(1, k^2, z) \beta_\mu \left[(|A|^2 \beta_\mu^2 + |B|^2) z + \frac{1}{4} \phi(1, k^2, z) (|C|^2 + |D|^2) (1 - \beta_\mu^2 \cos^2\theta) + 2\hat{m}_l(1 - k^2 + z) \text{Re}(BC^*) + 4\hat{m}_l^2 |C|^2 + 2\hat{m}_l \phi^{1/2}(1, k^2, z) \beta_\mu \text{Re}(AD^*) \cos\theta \right], \quad (\text{C2})$$

$$A \equiv \frac{1}{2}(1 - k^2) f_0(z) R_S, \\ B \equiv -\hat{m}_l C_{10} \left\{ f_+(z) - \frac{1 - k^2}{z} (f_0(z) - f_+(z)) \right\} + \frac{1}{2}(1 - k^2) f_0(z) R_P, \\ C \equiv C_{10} f_+(z), \quad (\text{C3})$$

$$D \equiv C_9^{\text{eff}} f_+(z) + 2C_7^{\text{eff}} \frac{f_T(z)}{1+k},$$

$$\phi(1, k^2, z) \equiv 1 + k^4 + z^2 - 2(k^2 + k^2 z + z),$$

$$\beta_\mu \equiv \left(1 - \frac{4\hat{m}_l^2}{z} \right).$$

In place of C_7 , one defines an effective coefficient $C_7^{(0)\text{eff}}$ which is renormalization scheme independent [42]:

$$C_7^{(0)\text{eff}}(\mu_b) = \eta^{16/23} C_7^{(0)}(\mu_W) + \frac{8}{3} (\eta^{14/23} - \eta^{16/23}) \times C_8^{(0)}(\mu_W) + C_2^{(0)}(\mu_W) \sum_{i=1}^8 h_i \eta^{\alpha_i} \quad (\text{C4})$$

where $\eta = \frac{\alpha_s(\mu_W)}{\alpha_s(\mu_b)}$, and

$$C_2^{(0)}(\mu_W) = 1, \quad C_7^{(0)}(\mu_W) = -\frac{1}{2} D'(x_l), \\ C_8^{(0)}(\mu_W) = -\frac{1}{2} E'(x_l); \quad (\text{C5})$$

the superscript (0) stays for leading logarithm approximation, which is not displayed in the text. Furthermore:

$$\begin{aligned}
\alpha_1 &= \frac{14}{23} & \alpha_2 &= \frac{16}{23} & \alpha_3 &= \frac{6}{23} & \alpha_4 &= -\frac{12}{23} \\
\alpha_5 &= 0.4086 & \alpha_6 &= -0.4230 & \alpha_7 &= -0.8994 \\
\alpha_8 &= -0.1456 & h_1 &= 2.996 & h_2 &= -1.0880 \\
h_3 &= -\frac{3}{7} & h_4 &= -\frac{1}{14} & h_5 &= -0.649 \\
h_6 &= -0.0380 & h_7 &= -0.0185 & h_8 &= -0.0057.
\end{aligned}
\tag{C6}$$

In the Naive dimensional regularization (NDR) scheme

one has

$$C_9(\mu) = P_0^{\text{NDR}} + \frac{Y(x_l)}{s_w^2} - 4Z(x_l) + P_E E(x_l), \tag{C7}$$

where $P_0^{\text{NDR}} = 2.60 \pm 0.25$ [42] and the last term is numerically negligible.

C_{10} is μ independent and is given by

$$C_{10} = -\frac{Y(x_l)}{s_w^2}. \tag{C8}$$

The normalization scale is fixed to $\mu = \mu_b \simeq 5 \text{ GeV}$.

-
- [1] G. Buchalla *et al.*, Eur. Phys. J. C **57**, 309 (2008).
[2] C. W. Chiang, arXiv:0808.1336.
[3] L. T. Handoko, C. S. Kim, and T. Yoshikawa, Phys. Rev. D **65**, 077506 (2002).
[4] A. Ali, T. Mannel, and T. Morozumi, Phys. Lett. B **273**, 505 (1991).
[5] T. Aaltonen *et al.* (CDF Collaboration), Phys. Rev. Lett. **100**, 101802 (2008).
[6] B. Aubert *et al.* (BABAR Collaboration), Phys. Rev. D **73**, 092001 (2006).
[7] A. Ishikawa *et al.* (Belle Collaboration), Phys. Rev. Lett. **91**, 261601 (2003).
[8] E. Lunghi, arXiv:hep-ph/0210379.
[9] P. Herczeg, Phys. Rev. D **27**, 1512 (1983); F. J. Botella and C. S. Lim, Phys. Rev. Lett. **56**, 1651 (1986); C. Q. Geng and J. N. Ng, Phys. Rev. Lett. **62**, 2645 (1989); G. Ecker and A. Pich, Nucl. Phys. **B366**, 189 (1991).
[10] V. Bashiry, M. Bayar, and K. Azizi, Phys. Rev. D **78**, 035010 (2008); A. Saddique, M. J. Aslam, and C. D. Lu, Eur. Phys. J. C **56**, 267 (2008).
[11] M. A. Paracha, I. Ahmed, and M. J. Aslam, Eur. Phys. J. C **52**, 967 (2007); I. Ahmed, M. A. Paracha, and M. J. Aslam, Eur. Phys. J. C **54**, 591 (2008).
[12] Y. G. Xu, R. M. Wang, and Y. D. Yang, Phys. Rev. D **74**, 114019 (2006).
[13] A. Ali, P. Ball, L. T. Handoko, and G. Hiller, Phys. Rev. D **61**, 074024 (2000); C. S. Huang, W. Liao, Q. S. Yan, and S. H. Zhu, Phys. Rev. D **63**, 114021 (2001); S. R. Choudhury, N. Gaur, A. S. Cornell, and G. C. Joshi, Phys. Rev. D **68**, 054016 (2003); A. S. Cornell and N. Gaur, J. High Energy Phys. 09 (2003) 030; S. R. Choudhury, N. Gaur, A. S. Cornell, and G. C. Joshi, Phys. Rev. D **69**, 054018 (2004); A. Mir, F. Tahir, and K. Ahmed, arXiv:0707.2268.
[14] H. C. Cheng and I. Low, J. High Energy Phys. 09 (2003) 051; 08 (2004) 061; I. Low, J. High Energy Phys. 10 (2004) 067.
[15] M. Blanke *et al.*, J. High Energy Phys. 01 (2007) 066.
[16] C. T. Hill, Phys. Lett. B **345**, 483 (1995); K. Lane and T. Eichten, Phys. Lett. B **352**, 382 (1995); K. Lane, Phys. Lett. B **433**, 96 (1998); G. Cvetic, Rev. Mod. Phys. **71**, 513 (1999).
[17] G. Buchalla, G. Burdman, C. T. Hill, and D. Kominis, Phys. Rev. D **53**, 5185 (1996).
[18] Z. J. Xiao *et al.*, Commun. Theor. Phys. **33**, 269 (2000); Z. H. Xiong and J. M. Yang, Phys. Lett. B **546**, 221 (2002).
[19] Z. H. Xiong and J. M. Yang, Nucl. Phys. **B602**, 289 (2001).
[20] C. T. Hill and E. H. Simmons, Phys. Rep. **381**, 235 (2003); **390**, 553(E) (2004).
[21] C. X. Yue, Y. P. Kuang, and G. R. Lu, J. Phys. G **23**, 163 (1997).
[22] S. L. Glashow, J. Iliopoulos, and L. Maiani, Phys. Rev. D **2**, 1285 (1970).
[23] H. J. He and C. P. Yuan, Phys. Rev. Lett. **83**, 28 (1999); G. Burdman, Phys. Rev. Lett. **83**, 2888 (1999).
[24] H. J. He, S. Kanemura, and C. P. Yuan, Phys. Rev. Lett. **89**, 101803 (2002).
[25] C. T. Hill, arXiv:hep-ph/9702320.
[26] C. X. Yue, L. H. Wang, and W. Ma, Phys. Rev. D **74**, 115018 (2006).
[27] A. K. Alok, A. Dighe, and S. U. Sankar, Phys. Rev. D **78**, 034020 (2008).
[28] T. Inami and C. S. Lim, Prog. Theor. Phys. **65**, 297 (1981); A. J. Buras, arXiv:hep-ph/9806471.
[29] W. M. Yao *et al.* (Particle Data Group), J. Phys. G **33**, 1 (2006).
[30] P. B. Mackenzie, arXiv:hep-ph/0606034.
[31] W. Loinaz and T. Takeuchi, Phys. Rev. D **60**, 015005 (1999); C. X. Yue, Y. P. Kuang, X. L. Wang, and W. B. Li, Phys. Rev. D **62**, 055005 (2000).
[32] A. A. Andrianov, P. Osland, A. A. Pankov, N. V. Romanenko, and J. Sirkka, Phys. Rev. D **58**, 075001 (1998); K. R. Lynch, S. Mrenna, M. Narain, and E. H. Simmons, Phys. Rev. D **63**, 035006 (2001).
[33] E. H. Simmons, Phys. Lett. B **526**, 365 (2002).
[34] R. S. Chivukula and E. H. Simmons, Phys. Rev. D **66**, 015006 (2002).
[35] B. Aubert *et al.* (BABAR Collaboration), Phys. Rev. Lett. **96**, 241802 (2006).
[36] Z. J. Xiao *et al.*, Eur. Phys. J. C **18**, 681 (2001).
[37] A. Birkedal, A. Noble, M. Perelstein, and A. Spray, Phys. Rev. D **74**, 035002 (2006); M. Asano, S. Matsumoto, N. Okada, and Y. Okada, Phys. Rev. D **75**, 063506 (2007); C. S. Chen, K. Cheung, and T. C. Yuan, Phys. Lett. B **644**,

- 158 (2007); M. Perelstein and A. Spray, Phys. Rev. D **75**, 083519 (2007).
- [38] J. Hubisz and P. Meade, Phys. Rev. D **71**, 035016 (2005); J. Hubisz *et al.*, J. High Energy Phys. 01 (2006) 135.
- [39] M. Blanke *et al.*, J. High Energy Phys. 12 (2006) 003.
- [40] J. Hubisz, S. J. Lee, and G. Paz, J. High Energy Phys. 06 (2006) 041; A. Freitas and D. Wyler, J. High Energy Phys. 11 (2006) 061; M. Blanke *et al.*, Phys. Lett. B **646**, 253 (2007).
- [41] A. Ali, E. Lunghi, C. Greub, and G. Hiller, Phys. Rev. D **66**, 034002 (2002).
- [42] A. J. Buras, M. Misiak, M. Munz, and S. Pokorski, Nucl. Phys. **B424**, 374 (1994).